Journal Pre-proofs

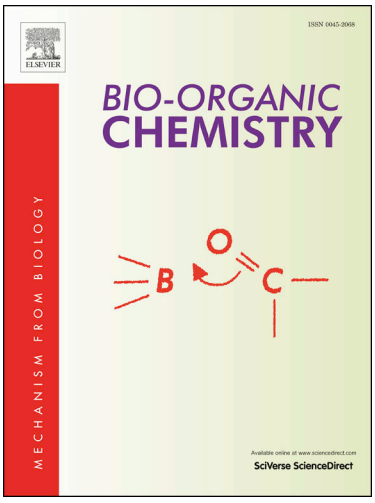

Synthesis, *In vitro* and *In silico* Screening of 2-Amino-4-Aryl-6-(phenylthio) pyridine-3,5-dicarbonitriles as Novel α-Glucosidase Inhibitors

Muhammad Ali, Khalid Mohammed Khan, Mohammad Mahdavi, Abdul Jabbar, Shahbaz Shamim, Uzma Salar, Muhammad Taha, Shahnaz Parveen, Bagher Larijani, Mohammad Ali Faramarzi

PII: S0045-2068(20)30479-X
DOI: https://doi.org/10.1016/j.bioorg.2020.103879
Reference: YBIOO 103879

To appear in: *Bioorganic Chemistry*

Received Date: 29 February 2020
Revised Date: 16 April 2020
Accepted Date: 22 April 2020

Please cite this article as: M. Ali, K. Mohammed Khan, M. Mahdavi, A. Jabbar, S. Shamim, U. Salar, M. Taha, S. Parveen, B. Larijani, M. Ali Faramarzi, Synthesis, *In vitro* and *In silico* Screening of 2-Amino-4-Aryl-6-(phenylthio) pyridine-3,5-dicarbonitriles as Novel α-Glucosidase Inhibitors, *Bioorganic Chemistry* (2020), doi: https://doi.org/10.1016/j.bioorg.2020.103879

Synthesis, *In vitro* and *In silico* Screening of 2-Amino-4-Aryl-6-(phenylthio) pyridine-3,5-dicarbonitriles as Novel *α*-Glucosidase Inhibitors

Muhammad Ali,[1] Khalid Mohammed Khan,[*1,2,3] Mohammad Mahdavi,[4] Abdul Jabbar,[5] Shahbaz Shamim,[1] Uzma Salar,[6] Muhammad Taha,[3] Shahnaz Parveen,[7] Bagher Larijani,[4] Mohammad Ali Faramarzi[8]

[1]*H. E. J. Research Institute of Chemistry, International Center for Chemical and Biological Sciences, University of Karachi, Karachi-75270, Pakistan*

[2]*Pakistan Academy of Sciences, 3-Constitution Avenue G-5/2, Islamabad, Pakistan*

[3]*Department of Clinical Pharmacy, Institute for Research and Medical Consultations (IRMC), Imam Abdulrahman Bin Faisal University, P.O. Box 31441, Dammam, Saudi Arabia*

[4]*Endocrinology & Metabolism Research Institute (EMRI), Tehran University of Medical Sciences, Tehran, Iran*

[5]*Department of Veterinary Biosciences, Melbourne Veterinary School, Faculty of Veterinary and Agricultural Sciences, The University of Melbourne, 250 Princes Highway, Werribee, Victoria 3030, Australia*

[6]*Dr. Panjwani Center for Molecular Medicine and Drug Research, International Center for Chemical and Biological Sciences, University of Karachi, Karachi-75270, Pakistan*

[7]*PCSIR Laboratories Complex, Karachi, Shahrah-e-Dr. Salimuzzaman Siddiqui, Karachi-75280, Pakistan*

[8]*Department of Pharmaceutical Biotechnology, Faculty of Pharmacy and Biotechnology Research Center, Tehran University of Medical Sciences, Iran*

Abstract: Inhibition of *α*-glucosidase enzyme is of prime importance for the treatment of diabetes mellitus (DM). Apart of many organic scaffolds, pyridine based compounds have previously been reported for wide range of bioactivities. The current study reports a series of pyridine based synthetic analogues for their *α*-glucosidase inhibitory potential assessed by *in vitro*, kinetics and *in silico* studies. For this purpose, 2-amino-4-aryl-6-(phenylthio)pyridine-3,5-dicarbonitriles **1-28** were synthesized and subjected to *in vitro* screening. Several analogs, including **1-3**, **7**, **9**, **11-14**, and **16** showed many folds increased inhibitory potential in comparison to the standard acarbose (IC_{50} = 750 ± 10 μM). Interestingly, compound **7** (IC_{50} = 55.6 ± 0.3 μM) exhibited thirteen-folds greater inhibition strength than the standard acarbose. Kinetic studies on most potent molecule **7** revealed a competitive type inhibitory mechanism. *In silico* studies have been performed to examine the binding mode of ligand (compound **7**) with the active site residues of *α*-glucosidase enzyme.

Keywords: Synthetic pyridine analogs; *α*-glucosidase inhibition *in vitro*, acarbose; structure-activity relationship; kinetics; *in silico* study

[*]*Corresponding Author*: khalid.khan@iccs.edu; drkhalidhej@gmail.com; Tel. 00922134824910; Fax. 00922134819018

Introduction

α-Glucosidase enzyme is located in the small intestine and responsible for breaking of carbohydrates which eventually results in the increased level of *α*-glucose in the blood [1-3]. Globally diabetes is considered to be one of the most serious threats to humans which can render severe health complications. Moreover, the most prevalent expressed form of this disease is type II diabetes [4]. Since 1980 to 2008, the number of individuals suffering from diabetes mellitus (DM) has expanded from 153 to 347 million around the globe. According to WHO, diabetes is considered to be the seventh most serious cause of mortality by 2030 [5,6]. Controlling the over-expression of *α*-glucosidase, is thought to be a way for the treatment of diabetes and other associated ailments such as increased body mass [7], gestational diabetes [8], and cardiovascular diseases [9]. A considerable way to treat the type 2 DM is to inhibit the intestinal *α*-glucosidase. Several *α*-glucosidase inhibitors based drugs such as acarbose, voglibose, and miglitol are available in the market for the treatment of type 2 DM but their adverse effects do not allow them to be the appropriate therapeutic agents for the cure of DM [10]. Scientist are still interested in the identification of antidiabetic agents based on natural and synthetic origins [11-16]. Mollica et. al. recognized that Turkish hazelnut contains high concentration of phenolic acids and flavonoids those have the ability to inhibit *α*-glucosidase enzyme. Similarly, they have also discovered novel peptides as attractive leads for the treatment of DM by performing computer aided virtual screening, followed by *in vitro*, pharmacokinetic evaluation [15,16]. It is essentially important to design new, safe, and better *α*-glucosidase inhibitors that could serve as an effective lead candidate for the better cure of DM.

Pyridine is six-membered aromatic heterocyclic organic compound, synthesized by treating ethyl acetoacetate, aldehyde, and ammonia which is known as Hantzsch pyridine synthesis. Pyridine and derivatives have acquired a significant position among the heterocyclic compounds due to their pharmacological and medicinal importance [17]. Pyridine is used in the synthesis of many drugs such as tripelennamine, mepyramine (antihistaminic drugs), sulfapyridine used for the treatment of bacterial and viral infections. Cicletanine is a furopyridine based antihypertensive drug with diuretic property [18]. Isoniazid is pyridine containing drug used for the treatment of tuberculosis [19]. In the recent past, we have reported the diversified synthetic pyridine centered molecules and their medicinal significance found to have *α*-glucosidase, *α*-amylase, *β*-glucuronidase, antioxidant, and antiglycation potential [20-24] (Figure-1). The encouraging results motivate us to synthesize a different type of pyridine analogues with several biologically

significant substituents to assess their efficacy. Herein, we are reporting the synthesis, *in vitro*, and *in silico* evaluation of 2-amino-4-aryl-6-(phenylthio) pyridine-3,5-dicarbonitriles **1-28**.

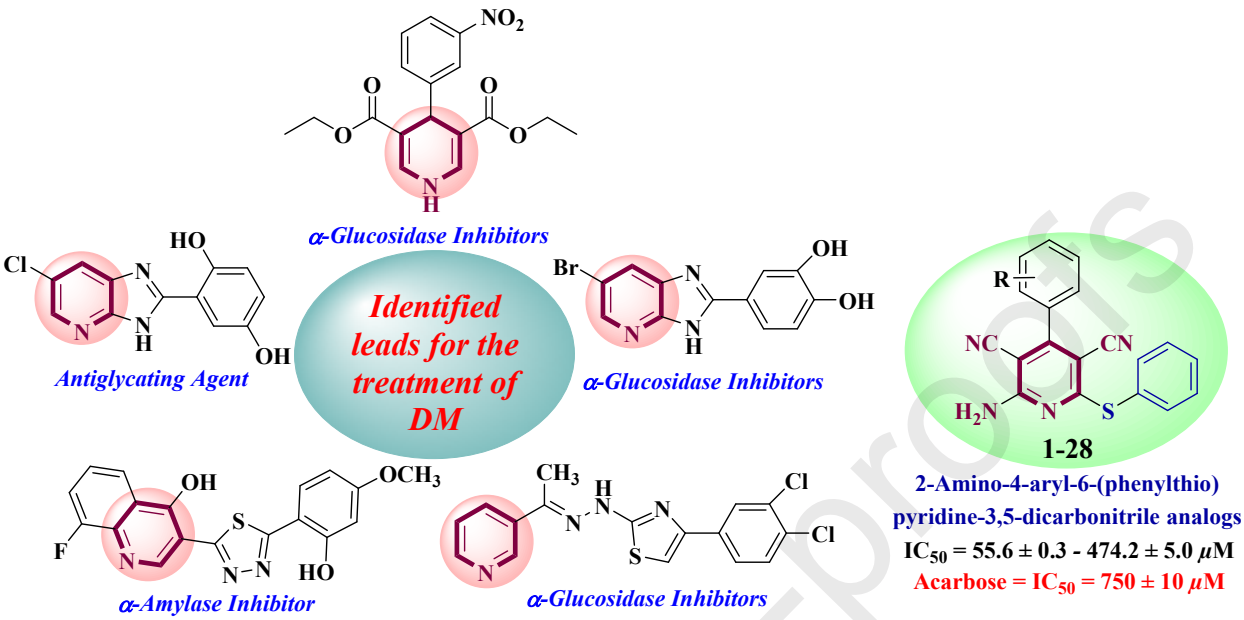

Figure-1: Rationale of the current study.

Results and Discussion

Chemistry

2-Amino-4-aryl-6-(phenylthio) pyridine-3,5-dicarbonitrile derivatives **1-28** were prepared by following reaction scheme. First, the reaction of different aryl aldehydes with malononitrile, catalyzed by triethyl amine to form the 2-arylidenemalononitrile which was monitored by TLC analysis. Then, 2-benzylidenemalononitrile intermediates were treated with thiophenol and malononitrile, in the presence of triethyl amine to afford products in good yields (Scheme-1). Intermediates as well as the final product formation were examined by thin layer chromatography (TLC system = Hexane:Ethyl acetate (8:2)).

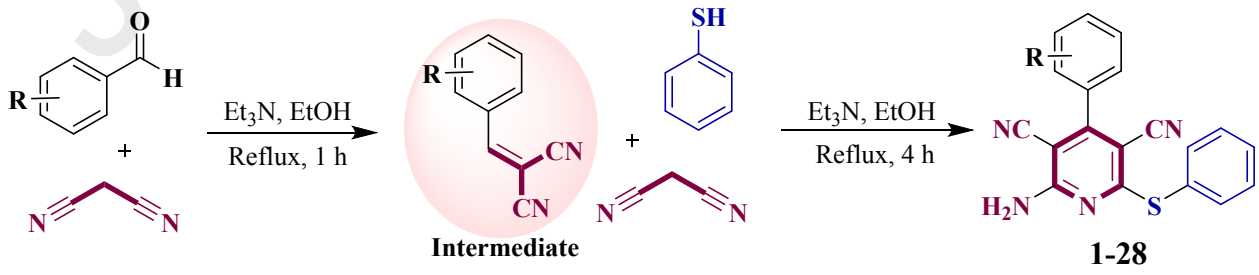

Scheme-1: Synthesis of 2-amino-4-aryl-6-(phenylthio) pyridine-3,5-dicarbonitriles **1-28**.

Chemical structures of all compounds were deduced by EI-MS and ^{1}H-NMR spectroscopic techniques. To the best of our knowledge eleven compounds **3**, **4**, **9-11**, **14**, **18**, **20**, **21**, **25**, and **26** are structurally new derivatives, so they were also subjected to HREI-MS and ^{13}C-NMR for further structural confirmation.

***In vitro* α-glucosidase inhibitory screening**

All synthetic 2-amino-4-aryl-6-(phenylthio) pyridine-3,5-dicarbonitriles were subjected for *in vitro* α-glucosidase inhibitory screening. It is worth mentioning that all molecules except **8**, **22**, **24**, **25**, and **28** were found to possess many folds increased inhibitory potential ranging from IC_{50} = 55.6 ± 0.3 to 474.2 ± 5.0 μM as compared to the standard acarbose (IC_{50} = 750.0 ± 10.0 μM) (Table-1).

Table-1: *In vitro* α-glucosidase inhibitory activities of pyridine derivatives **1-28**.

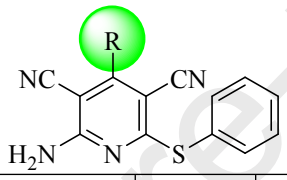

Comp. No.	R	α-Glucosidase Inhibitory Activity (μM ± SEM[a])	Comp.	R	α-Glucosidase Inhibitory Activity (μM ± SEM[a])
1	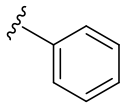	162.7 ± 1.7	**15**	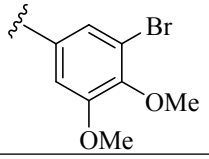	205.0 ± 2.5
2	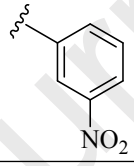	103.7 ± 0.9	**16**	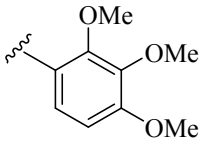	315.4 ± 3.6
3	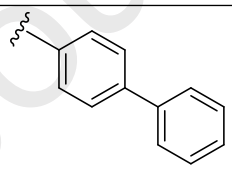	184.3 ± 2.1	**17**	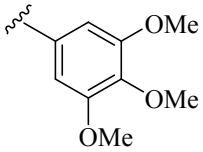	750 <
4	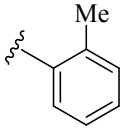	273.6 ± 3.1	**18**	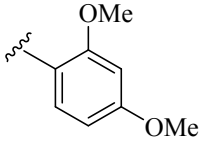	332.3 ± 3.9
5	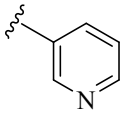	304.5 ± 3.5	**19**	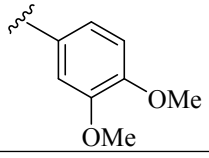	750 <

6	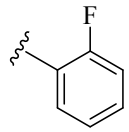	450.6 ± 4.7	**20**	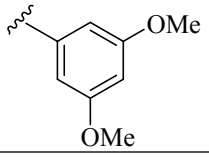	750 <
7	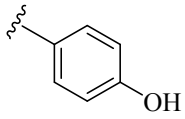	55.6 ± 0.3	**21**	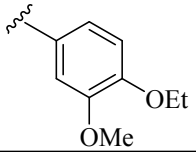	448.7 ± 5.5
8	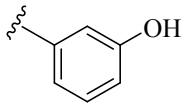	750 <	**22**	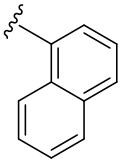	125.0 ± 1.0
9	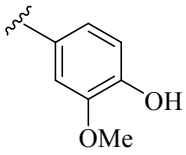	474.2 ± 5.0	**23**	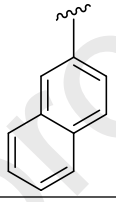	156.7 ± 1.6
10	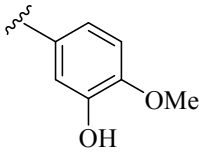	750 <	**24**	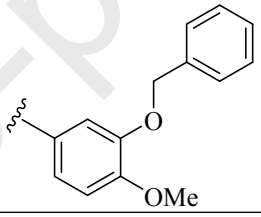	130.8 ± 1.1
11	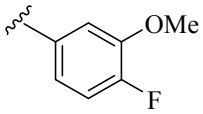	227.4 ± 2.8	**25**	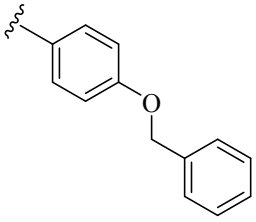	175.1 ± 1.9<
12	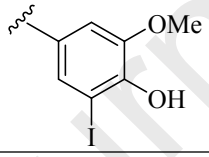	240.1 ± 2.9	**26**	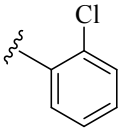	160.5 ± 1.7
13	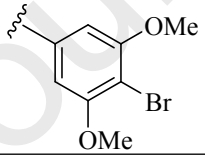	92.7 ± 0.7	**27**	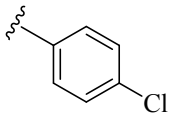	324.7 ± 3.8
14	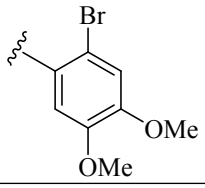	191.6 ± 2.3	**28**	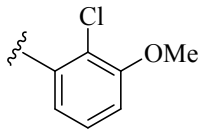	326.5 ± 3.8
Standard (Acarbose)[b]			750.0 ± 10.0		

SEM[a] (standard error mean); Acarbose[b] (Standard for α-glucosidase inhibitory activity).

Structure-activity relationship (SAR)

Albeit, all structural characteristics of synthetic analogs seem to have an indispensable role in the inhibitory potential but structure-activity relationship (SAR) has been established on the basis of varying substituents on the phenyl ring "R".

Compound **1** (IC_{50} = 162.7 ± 1.7 μM) with unsubstituted phenyl ring found to be four-folds more active than the standard acarbose (IC_{50} = 750 ± 10 μM). Incorporation of substituents significantly affected the inhibitory potential. Such as compound **2** (IC_{50} = 103.7 ± 0.9 μM) with *m*-nitro substitution at phenyl ring, showed significant increased inhibitory potential as compared to compound **1** and the standard acarbose. The enhanced inhibition by compound **2** might be due to the electron-withdrawing effect of the nitro group which makes the ring more polarizable to interact with the active binding site of an enzyme. However, in some cases substitution leads to the decline in the inhibitory potential as observed in case of *o*-methyl and *o*-fluoro substituted compounds **4** (IC_{50} = 273.6 ± 3.1 μM) and **6** (IC_{50} = 450.6 ± 4.7 μM), respectively. The decreased activity might be due to the occupied *ortho* position which may create some steric hindrance during binding. However, it is still worth-mentioning that compound **4** and **6** are much better active than the standard acarbose. One exceptional derivative **5** (IC_{50} = 304.5 ± 3.5 μM) having pyridine ring instead of phenyl as "R", revealed two-fold more potent inhibitory potential than the standard acarbose (Figure-2) which gave us an idea to explore the effect of substituted pyridine as "R" on the inhibitory potential in the near future.

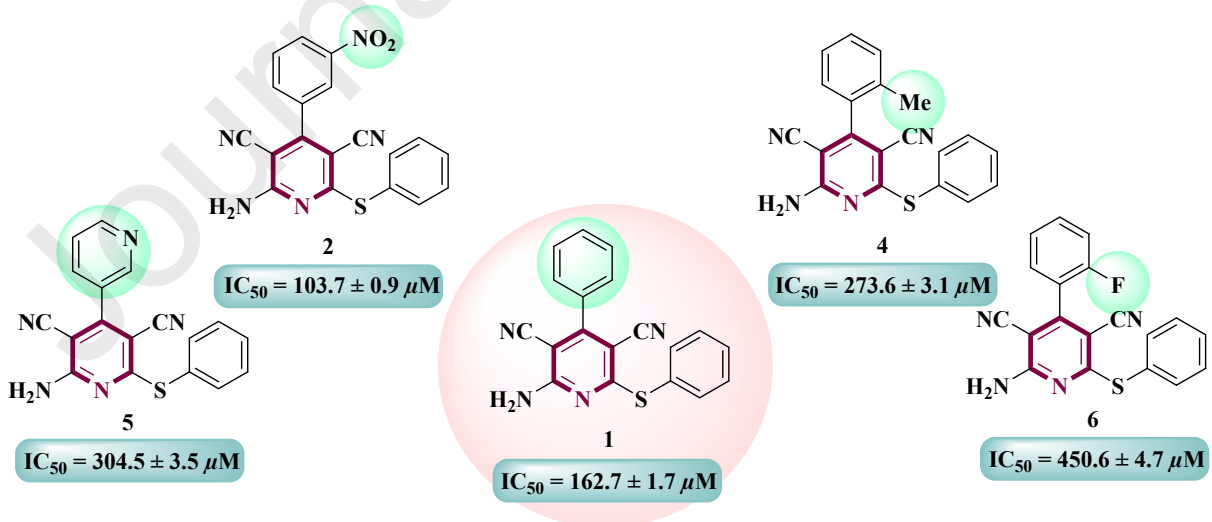

Figure-2: Structure-activity relationship of compounds **1**, **2**, **4-6**.

p-Hydroxy substituted compound **7** (IC_{50} = 55.6 ± 0.3 μM), the most potent member of this synthetic library, identified as thirteen-fold more potent in comparison to the standard acarbose (IC_{50} = 750 ± 10 μM). This promising inhibition potential could be attributed to the hydroxy group, specifically at the *para* position, might be the most appropriate position to bind with the active site of an enzyme. *m*-Hydroxy substituted residue **8** (IC_{50} = 750 ± 10 μM) with the same structural feature but the different position of hydroxy group, resulted in several folds decreased inhibitory potential suggests that position of a substituent at a specific position is very important to bind with the active site of an enzyme. Comparison of analog **9** (IC_{50} = 474.2 ± 5.0 μM) with compound **7**, having almost identical structure but only incorporation of methoxy group adjacent to hydroxy, resulted in decrease of inhibitory strength might be due to factor of steric hindrance by the methoxy substituent adjacent to hydroxy. Furthermore, compound **10** (IC_{50} = 750< μM) distinctly similar to compound **9** but with reverted positions of hydroxy and methoxy substituents, displayed significantly lower activity as compared to compound **9** but similar inhibitory strength to the standard acarbose. Activity of derivative **9** can be compared with another derivative **11** (IC_{50} = 227.4 ± 2.8 μM) having fluoro group instead of hydroxy, revealed enhanced inhibitory strength which suggests that being an electronegative group, fluoro is playing a critical role in the efficacy of this analogue. Similarly, compound **12** (IC_{50} = 240.1 ± 2.9 μM) with an additional iodo group at *meta* position also showed almost two-folds enhanced inhibitory strength, compared to compound **9** which reveals the significance and active participation of halogen group in the activity (Figure-3).

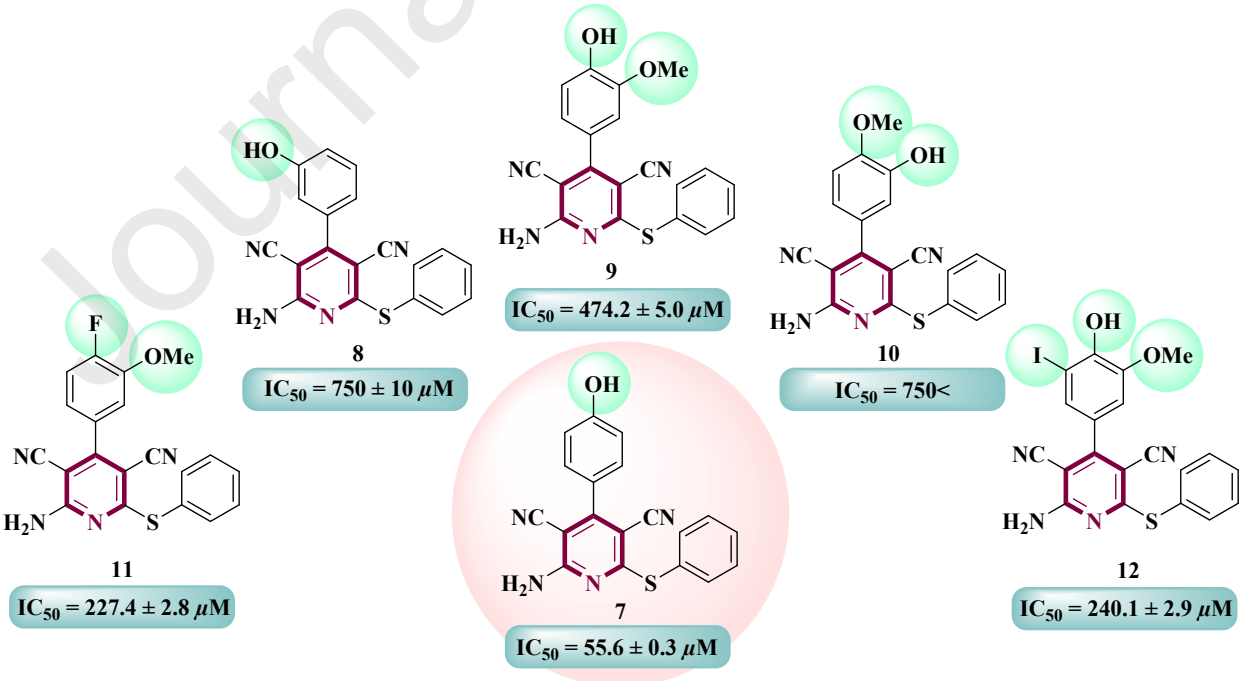

Figure-3: Structure-activity relationship of compounds **7-12**.

Among the di- and tri-alkoxy substituted analogs, compound **13** (IC_{50} = 92.7 ± 0.7 μM) with di-methoxy substitutions at two *meta* positions and a bromo at *para*, found to be the second most potent molecule of this series as well as seven-times more active than the standard acarbose. Its good inhibitory potential might be due to symmetrical substitution pattern which makes it favorable to bind with the enzyme. Replacement of bromo with another methoxy as in case of compound **17** (IC_{50} = 750< μM) leads to a decline in the inhibitory potential which revealed a crucial role of bromo group in inhibition of α-glucosidase. However, lack of bromo group in compound **20** (IC_{50} = 750< μM) also leads to decreased inhibition potential. Similarly, replacement of bromo and one of the methoxy as in cases of compounds **14** (IC_{50} = 191.6 ± 2.3 μM) and **15** (IC_{50} = 205.0 ± 2.5 μM) brings out the decline in the inhibitory strength as compared to compound **13** which gives the perception that switching of bromo position actually drives away the inhibition potential to a considerable extent and bromo group at *para* position is suitable to interact with the binding pocket of enzyme. Tri-methoxy substituted compound **16** (IC_{50} = 315.4 ± 3.6 μM) also showed more than two-fold increased inhibitory potential. Regretfully, tri-methoxy substituted compound **17** didn't show activity comparable to compound **16** might be due to not satisfying the conformational requirement to bind with the active site of α-glucosidase. Activity of analog **16** can be compared with residue **18** (IC_{50} = 332.3 ± 3.9μM) having almost similar structural feature but lack of one methoxy at *meta* position, displayed a slight decreased in inhibitory strength which shows that *m*-methoxy is not worth important for the inhibitory potential. Similarly, lack of *o*-methoxy in case of compound **19** (IC_{50} = 750< μM) displayed a sharp decline in the inhibitory strength as compared to compound **16** which indicates that the *ortho* position has worth importance in this activity. Activity comparison of compound **19** (IC_{50} = 750< μM) with **21** (IC_{50} = 448.7 ± 5.5 μM) revealed that insertion of ethoxy instead of methoxy at *para* position lifted up the inhibitory potential up to a good extent (Figure-4).

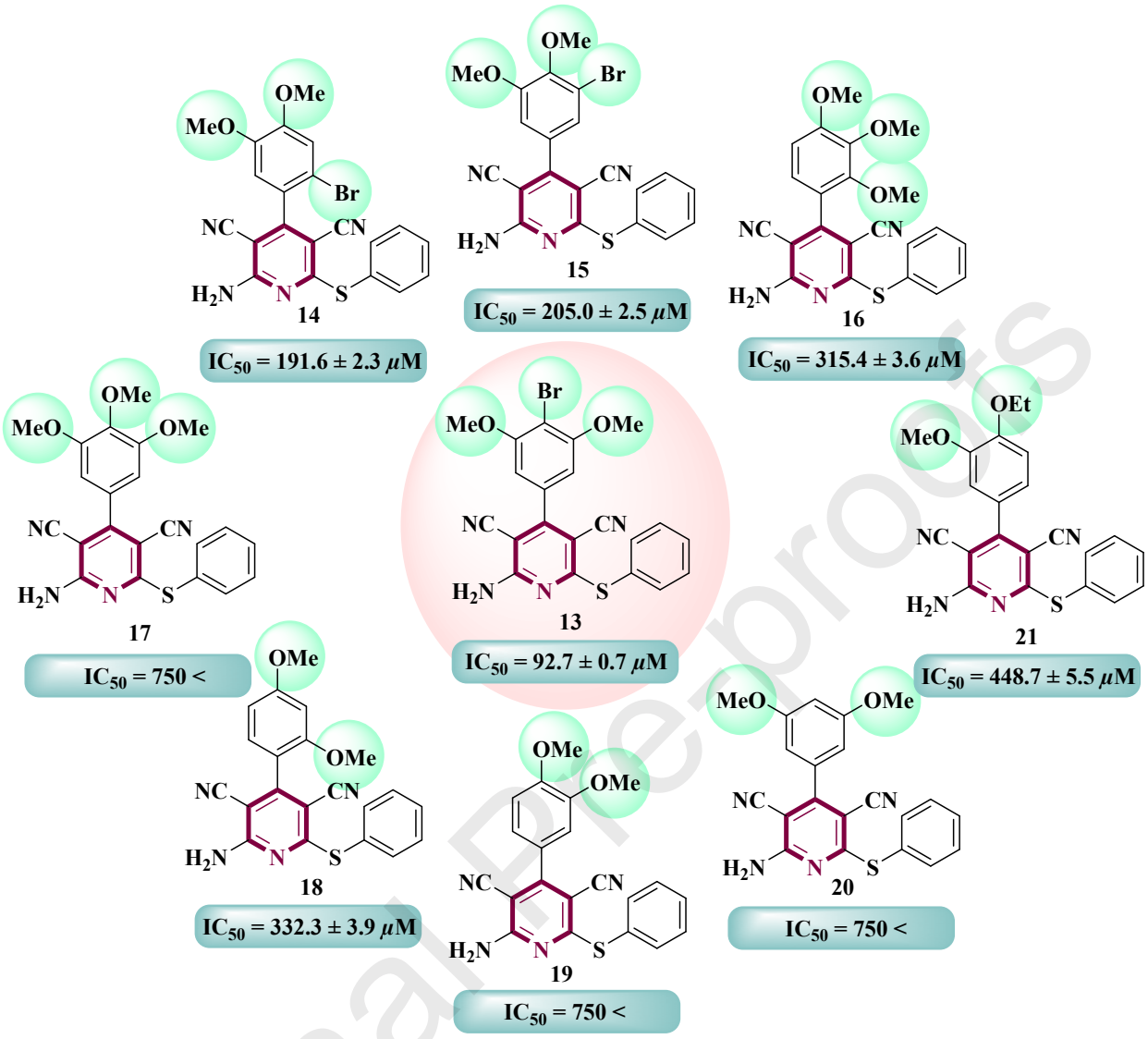

Figure-4: Structure-activity relationship of compounds **13-21**.

Compounds **3** and **22-25** with extended conjugation showed multifold enhanced inhibitory strength in the range of IC_{50} = 125.0 ± 1.0 - 184.3± 2.1 μM as compared to the standard acarbose (IC_{50} = 750 ± 10μM). Amongst them, compound **22** (IC_{50} = 125.0 ± 1.0μM) having the 1-naphthyl substitution was found to be six-fold more potent than standard and interestingly the fourth most potent molecule of this library. The considerable inhibition strength of compound **22** possibly due to the interaction of the extended π-electronic system with the active site of enzyme which resulted in the significant inhibition. Similarly, analog **23** (IC_{50} = 156.7 ± 1.6μM) with 2-naphthyl substitution also showed many folds enhanced inhibition potential. The inhibition strength of compound **23** is slightly lower than the compound **22** that could occur only due to some conformational differences. Furthermore, 3- benzyloxy-4-methoxy substituted compound **24** (IC_{50}

= 130.8 ± 1.1μM) is amongst the most potent member of this library. Its potent inhibitory strength might be due to combined effects of methoxy and benzyloxy group on inhibition. However, switching of benzyloxy to *para* position and absence of methoxy group as in case of compound **25** (IC_{50} = 175.1 ± 1.9 μM) leads to decrease in the inhibition potential which suggests that the position of benzyloxy and presence of methoxy group plays an important role in the inhibitory potential. Exceptionally, compound **3** (IC_{50} = 184.3± 2.1μM) with a biphenyl ring has also displayed four-folds more inhibition potential as compared to the standard, most probably due to extended conjugation which makes it better interact with the active site of an enzyme (Figure-5).

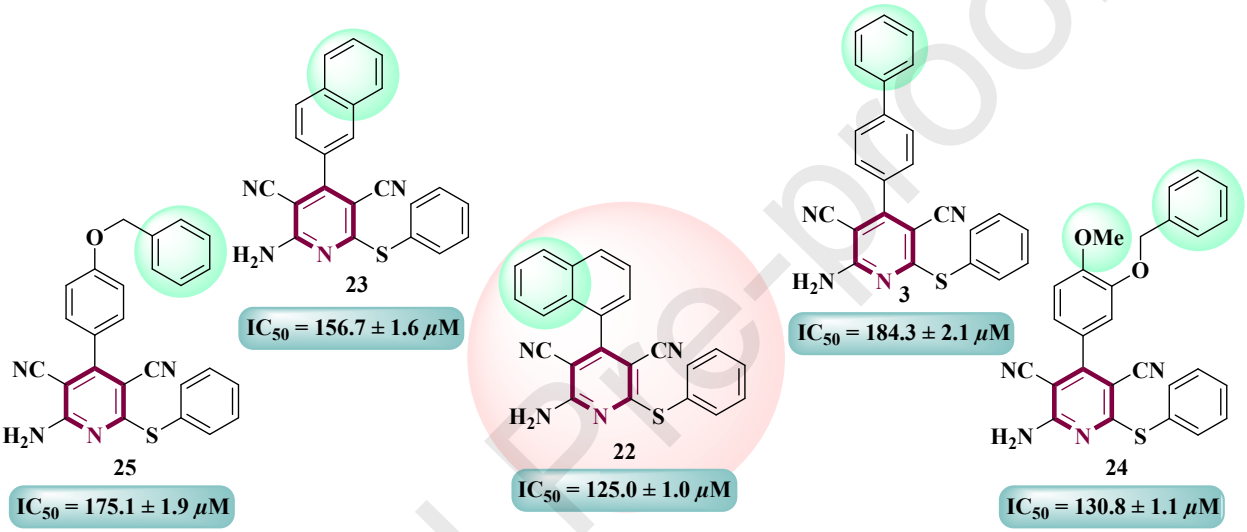

Figure-5: Structure-activity relationship of compounds **3**, **22-25**.

Amongst the chloro substituted derivatives, *o*-chloro substituted compound **26** (IC_{50} = 160.5 ± 1.7 μM) exhibited four-folds enhanced activity as compared to the standard acarbose (IC_{50} = 750 ± 10 μM). Switching of chloro group from *ortho* to *para* position as in case of derivative **27** (IC_{50} = 324.7 ± 3.8 μM) results in a two-fold decreased activity which indicates the *ortho* position is favorable for the chloro group to interact well with the active site of an enzyme. Incorporation of methoxy next to chloro in compound **28** (IC_{50} = 326.5 ± 3.8μM) leads to a two-fold decline in the inhibitory power might be creating the steric hindrance for the chloro group to interact with the active site residues (Figure-6).

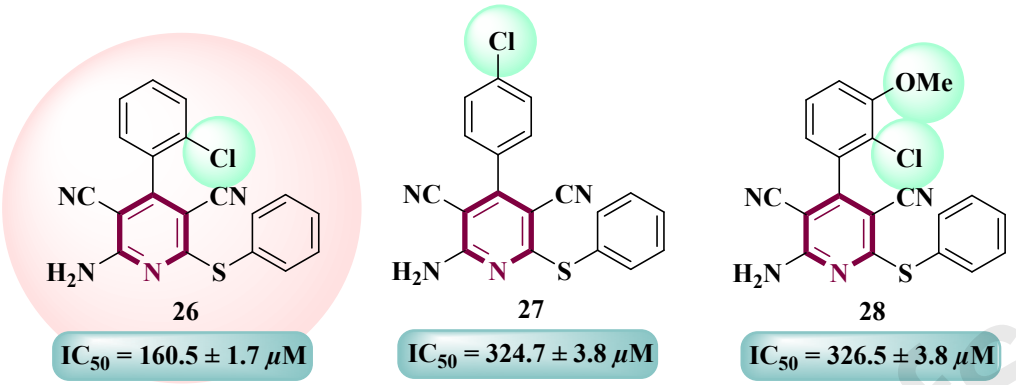

Figure-6: Structure-activity relationship of compounds 26-28

Limited SAR suggested that the halogens Br, F, Cl, and I and *p*-hydroxy substitutions played an important role in the inhibition potential. Furthermore, an extended conjugation also takes part in enhancing the strength of α-glucosidase inhibition.

Enzyme kinetic studies of α-glucosidase inhibition

Mode of inhibition of the most potent analog **7** was inspected contrary to α-glucosidase activity with different concentrations of the substrate which is *p*-nitrophenyl α-D-glucopyranoside (2-10 mM), in the absence and presence of sample (compound **7**) at different concentrations (0, 15, 35, and 55 μM). A Lineweaver-Burk plot was generated to ascertain the type of inhibition. The Michaelis-Menten constant (K_m) value was determined from the plot between reciprocal of the substrate concentration (1/[S]) and reciprocal of enzyme rate (1/V) over various inhibitor concentrations. Experimental inhibitor constant (K_i) value was determined by secondary plots of the inhibitor concentration [I] versus K_m.

According to (Figure-7a), the Lineweaver-Burk plot displayed a gradual increase in K_m value and no change in V_{max} with the increase of inhibitor concentration which indicates a competitive type inhibition. The results show that residue **7** compete with the substrate to bind with the active site of an enzyme. Furthermore, the plot of the K_m versus different concentration of inhibitor gave an approximation of the inhibition constant, K_i of 53 μM (Figure-7b).

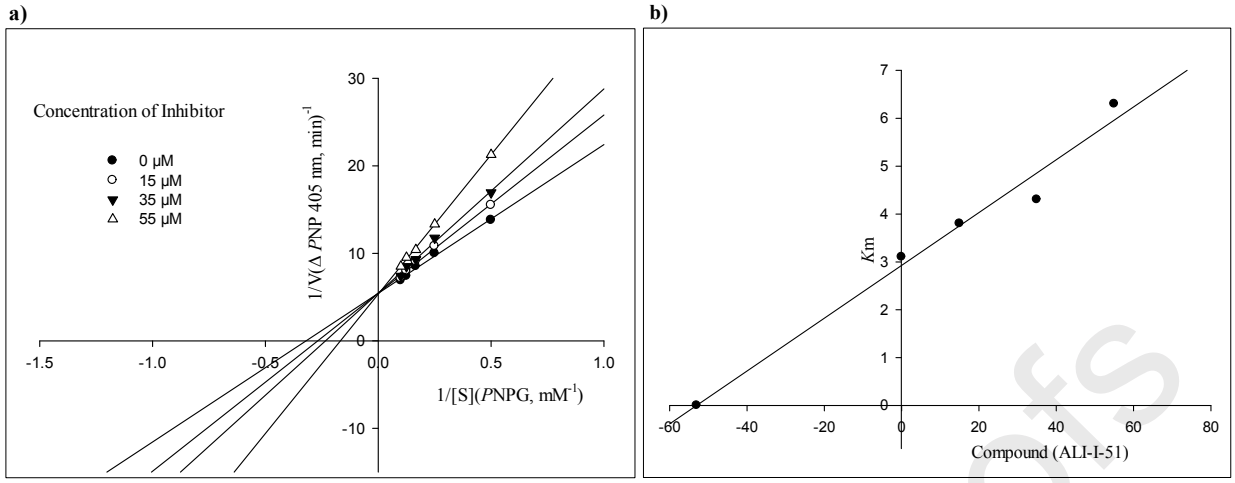

Figure-7: Kinetics of α-glucosidase inhibition by compound (**7**). (a) The Lineweaver-Burk plot in the absence and presence of different concentrations of compound (**7**); (b) The secondary plot between K_m and various concentrations of compound (**7**). Note: ALI-I-51 = Compound **7**

Docking study

Docking study was performed using Autodock Tools (version 1.5.6) in order to elucidate the interaction modes of the synthetic analogs in the α-glucosidase active site. Since the crystallographic structure of α-glucosidase from *S. cerevisiae* (target enzyme in α-glucosidase inhibition assay) do not report yet, we constructed modeled α-glucosidase by using the crystal structure of *S. cerevisiae* isomaltase that has 71% identity and 84% similarity with *S. cerevisiae* α-glucosidase [25]. Superimposition structure of standard inhibitor acarbose and most potent analog **7** in the active site of modeled α-glucosidase is shown in Figure-8.

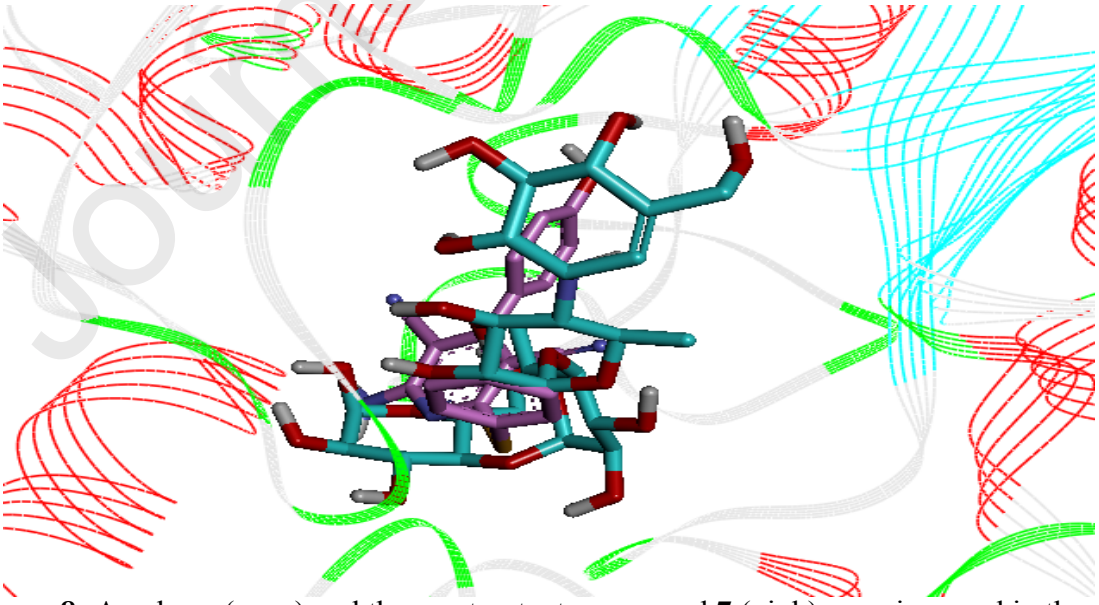

Figure-8: Acarbose (cyan) and the most potent compound **7** (pink) superimposed in the active site pocket of modeled α-glucosidase.

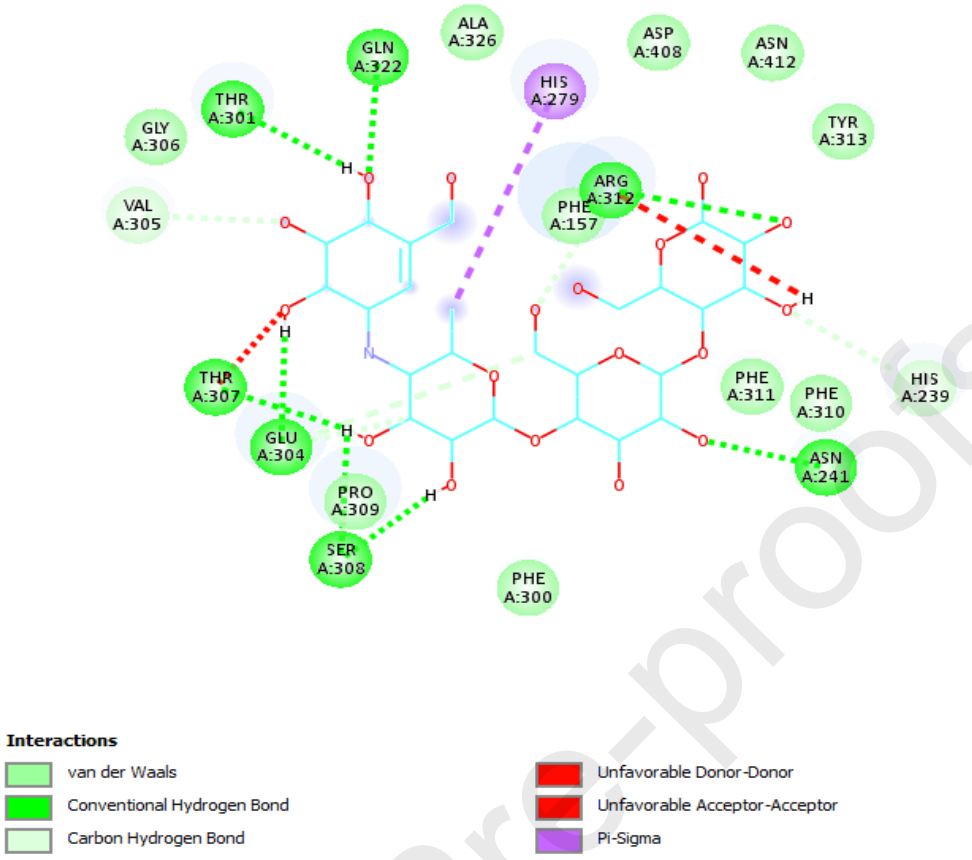

Figure-9: Docked conformer of acarbose in the active site of *α*-glucosidase.

Figure-9 shows that acarbose interacted with the active site residues Asn241, Ser308, Thr301, Glu304, Thr307, Arg312, and Gln322 *via* hydrogen bonds and residue His279 *via* hydrophobic interaction. Furthermore, it also created weak interactions with active site residues such as His239 and Val305.

The most active compound **7** interacted with residues Arg312, Glu304, His239, Phe157, His279, Phe300, and Gln350 (Figure-10a). Sulfur unit of 6-(phenylthio) moiety interacted with His239 and phenyl ring of this moiety interacted with Glu304 and Arg312 *via* a *π*-anion and a hydrophobic interaction, respectively. Arg312 also formed a hydrophobic interaction with the pyridine ring. 2-Amino and 5-cyano substituents of the pyridine ring created two hydrogen bonds with Phe157 and His279. Furthermore, 4-hydroxyphenyl moiety of compound **7** formed a *π*-*π* hydrophobic interaction with Phe300 *via* phenyl ring and a hydrogen bond with Gln350 *via* hydroxyl substituent.

The second most active compound **13** established three hydrogen bonds with Asp408, Arg312, and Asn241 through 2-amino and 3-cyano substituents of pyridine ring and 3-methoxy group of 4-bromo-3,5-dimethoxyphenyl moiety, respectively (Figure-10b). Pyridine ring and phenyl ring of 4-bromo-3,5-dimethoxyphenyl moiety also formed hydrophobic interactions with Arg312. The latter moiety also established hydrophobic interactions with His239 *via* 4-bromo group and phenyl ring as well as weak interactions with Glu304 and Ser308 *via* 5-mertoxy group. 6-(Phenylthio) moiety of compound **9** interacted with Phe158 (π-sulfur) and Asp349 (π-anion).

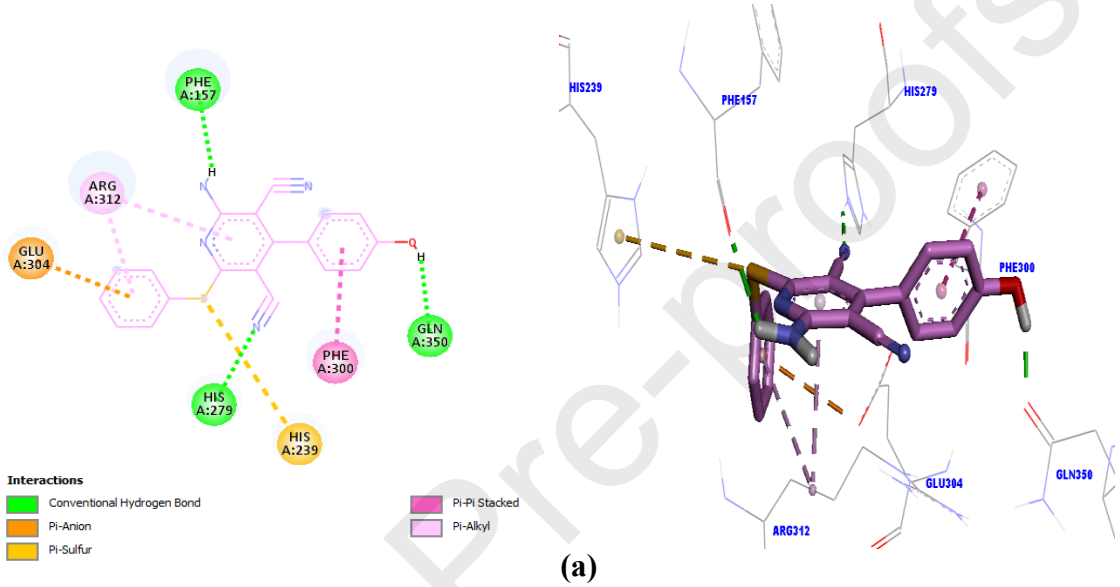

(a)

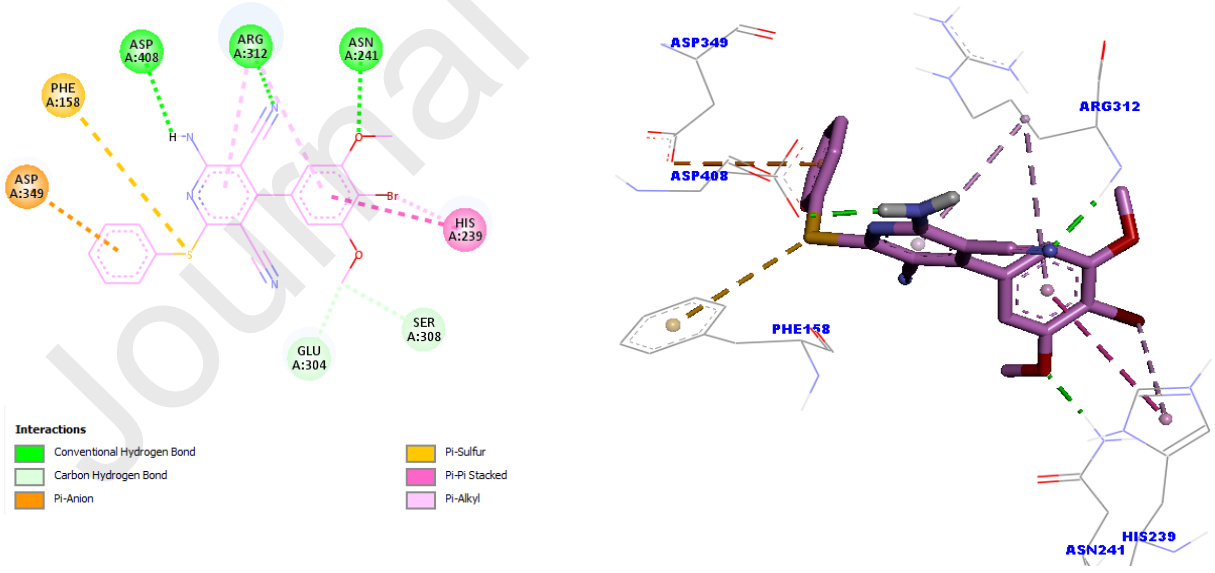

(b)

Figure-10: Docked conformer of the most potent compounds **7** (a) and **13** (b) in the active site of α-glucosidase enzyme.

Conclusion

This piece of research work describes the synthesis and *in vitro* screening of diversely functionalized pyridine derivatives for α-glucosidase inhibitory activity. Kinetics and molecular docking studies were conducted on most potent compounds to support the findings. It was found that many compounds displayed multifold enhanced inhibitory strength than the standard acarbose, especially, halogens Br, F, Cl, and I and *p*-hydroxy substituted compounds as well as compounds with extended conjugation. Kinetic studies of the most potent analogue revealed a competitive type of inhibition. Docking studies identified many structural features that played important role during binding with the active site of enzyme.

Experimental

Materials and Methods

Reagents were purchased from Sigma-Aldrich, USA and were of analytical grades. Thin-layer chromatography was performed on pre-coated silica gel, GF-254. Spots were visualized under ultraviolet light at 254 and 366 nm. Mass spectra were recorded on electron impact (EI) on MAT 312 and MAT 113D mass spectrometers. The ^{1}H- and ^{13}C-NMR were recorded on Bruker AM machines, operating at 300 and 400 MHz. The chemical shift values are presented in ppm (δ) relative to tetramethylsilane (TMS) as an internal standard and the coupling constant (J) are in Hz. Symbols in NMR description such as s, d, t, dd, m, and ovp, corresponds to singlet, doublet, triplet, doublet of doublet, multiplet, and overlapping multiplet, respectively.

General procedure for the syntheses of functionalized 2-amino-4-(substituted)phenyl-6-phenylsulfanylpyridine-3,5-dicarbonitriles 1-28

Malononitrile (1 mmol) was first dissolved in EtOH (7 mL) into a 100 mL round-bottomed flask, than aryl aldehyde (1 mmol) was added into it followed by 3 drops of triethylamine. The reaction mixture was refluxed for 1 h and progress was monitored *via* TLC analysis (Hexane and Ethyl acetate (8:2)). After intermediate formation, malononitrile (1 mmol), thiophenol (1 mmol), and triethylamine (3 drops) were added in the reaction mixture and refluxed for approximately 4 h and course of the reaction was monitored by TLC analysis. On completion, reaction mixture was allowed to cool to room temperature which resulted to precipitates formation. The crude product was collected by filtration and crystallized from EtOH to get the pure product. The purity of the

final products was checked by TLC analysis in different solvent systems to ensure absence of any residual impurity and the products were found to be pure.

2-Amino-4-phenyl-6-(phenylthio)pyridine-3,5-dicarbonitrile (1) [26]

Yellow Solid; Yield: 72%; M.P.: 255-257 °C; ^{1}H-NMR (400 MHz, DMSO-d_6) δ 7.78 (s, 2H, NH), 7.61 (ovp, 8H, H-2, H-3, H-4, H-5, H-6, H-3′, H-4′, H-5′), 7.50 (ovp, 2H, H-2′, H-6′); EI MS *m/z* (% rel. abund.): 328 (M^+, 96), 327 (100), 295 (4), 284 (6), 251 (2), 165 (9), 138 (2), 109 (4), 77 (6), 44 (16).

2-Amino-4-(3-nitrophenyl)-6-(phenylthio)pyridine-3,5-dicarbonitrile (2) [27]

Brown Solid; Yield: 55%; M.P.: 215-216 °C; ^{1}H-NMR (300 MHz, DMSO-d_6) δ 8.50 (s, 1H, H-2), 8.44 (dd, $J_{4,2}$ = 1.6 Hz, $J_{4,5}$ = 10.8 Hz, 1H, H-4), 8.06 (d, $J_{6,5}$ = 10.4 Hz, 1H, H-6), 7.92 (ovp, 3H, H-5, NH), 7.61 (ovp, 2H, H-3′, H-5′), 7.51 (ovp, 3H, H-2′, H-4′, H-6′); EI MS *m/z* (% rel. abund.): 373 (M^+, 100), 372 (72), 343 (11), 326 (40), 310 (5), 266 (3), 190 (3), 163 (5), 109 (6).

4-([1,1'-Biphenyl]-4-yl)-2-Amino-6-(phenylthio)pyridine-3,5-dicarbonitrile (3)

Off White Solid; Yield: 60%; M.P.: 175-177 °C; ^{1}H-NMR (400 MHz, DMSO-d_6) δ 7.89 (d, $J_{9,8}$ = $J_{11,12}$ = 8.0 Hz, 2H, H-9, H-11), 7.81 (s, 1H, NH), 7.79 (d, $J_{8,9}$ = $J_{12,11}$ = 7.6 Hz, 2H, H-8, H-12), 7.66 (d, $J_{2,3}$ = $J_{6,5}$ = 8.4 Hz, 2H, H-2, H-6), 7.62 (ovp, 2H, H-3′, H-5′), 7.53 (ovp, 5H, H-3, H-5, H-2′, H-4′, H-6′), 7.37 (t, $J_{10(9,11)}$ = 7.6 Hz, 1H, H-10); ^{13}C-NMR (DMSO-d_6, 100 MHz): δ_C 166.1, 159.6, 158.2, 141.9, 138.8, 134.7, 134.7, 132.8, 129.6, 129.4, 129.4, 129.1, 129.1, 129.0, 129.0, 128.1, 127.1, 126.8, 126.8, 126.8, 126.8, 115.3, 115.0, 93.2, 86.9; EI MS *m/z* (% rel. abund.): 404 (M^+, 100), 403 (93), 327 (16), 241 (3), 202 (7), 152 (3), 108 (2), 76 (5); HRESI-MS Calcd for $C_{25}H_{16}N_4S$: *m/z* = 404.1086, Found 404.1096.

2-Amino-6-(phenylthio)-4-(*o*-tolyl)pyridine-3,5-dicarbonitrile (4)

White Solid; Yield: 55%; M.P.: 185-187 °C; ^{1}H-NMR (400 MHz, DMSO-d_6) δ 7.83 (s, 2H, NH), 7.62 (ovp, 2H, H-3′, H-5′), 7.50 (ovp, 3H, H-2′, H-4′, H-6′), 7.45 (ovp, 2H, H-11, H-12), 7.44 (t, $J_{10(9,11)}$ = 7.6 Hz, 1H, H-10), 7.29 (d, $J_{9,10}$ = 7.6 Hz, 1H, H-9), 2.17 (s, 3H, CH_3); ^{13}C-NMR (DMSO-d_6, 125 MHz): δ_C 165.8, 159.4, 159.0, 134.7, 134.7, 134.6, 133.9, 130.4, 129.9, 129.6, 129.4, 129.4, 128.1, 127.0, 127.0, 126.2, 114.8, 114.5, 93.8, 87.6; EI MS *m/z* (% rel. abund.): 342 (M^+, 100), 341 (76), 327 (26), 265 (87), 238 (5), 206 (5), 179 (8), 152 (7), 140 (6), 77 (7)); HRESI-MS Calcd for $C_{20}H_{14}N_4S$: *m/z* = 342.0943, Found 342.0939.

2'-Amino-6'-(phenylthio)-[3,4'-bipyridine]-3',5'-dicarbonitrile (5) [28]

Light Yellow Crystalline Solid; Yield: 60%; M.P.: 305-306 °C; ^{1}H-NMR (400 MHz, DMSO-d_6) δ 8.77 (ovp, 2H, H-2, H-4), 8.05 (dd, $J_{6,2}$ = 2.0 Hz, $J_{6,5}$ = 8.0 Hz, 1H, H-6), 7.89 (s, 2H, NH), 7.64 (ovp, 3H, H-5, H-3′, H-5′), 7.50 (ovp, 3H, H-2′, H-4′, H-6′); EI MS *m/z* (% rel. abund.): 329 (M^+, 94), 328 (100), 312 (2), 301 (4), 285 (4) 263 (2), 166 (3), 139 (2), 109 (4), 77 (4).

2-Amino-4-(2-fluorophenyl)-6-(phenylthio)pyridine-3,5-dicarbonitrile (6) CAS # 391666-95-8

Yellow Solid; Yield: 55%; M.P.: 195-197 °C; ^{1}H-NMR (400 MHz, DMSO-d_6) δ 7.90 (s, 2H, NH), 7.67 (ovp, 5H, H-3, H-4, H-6, H-3′, H-5′), 7.50 (ovp, 3H, H-2′, H-4′, H-6′), 7.43 (t, $J_{5(4,6)}$ = 7.6 Hz, 1H, H-5); EI MS *m/z* (% rel. abund.): 346 (M^+, 98), 345 (100), 328 (12), 327 (41), 320 (6), 302 (7), 291 (2), 251 (2), 183 (9), 173 (6), 163 (3), 146 (5), 136 (4), 109 (6), 77 (6).

2-Amino-4-(4-hydroxyphenyl)-6-(phenylthio)pyridine-3,5-dicarbonitrile (7) [29]

Brown Solid; Yield: 55%; M.P.: 312-314 °C; ^{1}H-NMR (400 MHz, DMSO-d_6) δ 10.05 (s, 1H, OH), 7.69 (s, 2H, NH), 7.60 (ovp, 2H, H-3′, H-5′), 7.49 (ovp, 3H, H-2′, H-4′, H-6′), 7.39 (d, $J_{2,3}$ = $J_{6,5}$ = 8.8 Hz, 2H, H-3, H-5), 6.92 (d, $J_{3,2}$ = $J_{5,6}$ = 8.4 Hz, 2H, H-3, H-5); EI MS *m/z* (% rel. abund.): 344 (M^+, 91), 343 (100), 327 (11), 300 (4), 181 (4), 109 (3).

2-Amino-4-(3-hydroxyphenyl)-6-(phenylthio)pyridine-3,5-dicarbonitrile (8) [30]

White Crystalline Solid; Yield: 58%; M.P.: 335-337 °C; ^{1}H-NMR (400 MHz, DMSO-d_6) δ 9.86 (s, 1H, OH), 7.73 (s, 2H, NH), 7.60 (ovp, 2H, H-3′, H-5′), 7.49 (ovp, 3H, H-2′, H-4′, H-6′), 7.36 (t, $J_{5(4,6)}$ = 8.0 Hz, 1H, H-5), 6.95 (d, $J_{2,6}$ = 0.8 Hz, 1H, H-2), 6.93 (dd, $J_{6,2}$ = 0.8 Hz, $J_{6,5}$ = 6.4 Hz, 1H, H-6), 6.89 (dd, $J_{4,6}$ = 1.6 Hz, $J_{4,5}$ = 10.4 Hz, 1H, H-4); EI MS *m/z* (% rel. abund.): 344 (M^+, 100), 343 (85), 327 (16), 286 (4), 161 (45), 160 (83), 133 (11), 104 (10), 77 (9).

2-Amino-4-(4-hydroxy-3-methoxyphenyl)-6-(phenylthio)pyridine-3,5-dicarbonitrile (9) [31]

White Solid; Yield: 62%; M.P.: 227-229°C; ^{1}H-NMR (300 MHz, DMSO-d_6) δ 9.67 (s, 1H, OH), 7.69 (s, 2H, NH), 7.60 (ovp, 2H, H-3′, H-5′), 7.49 (ovp, 3H, H-2′, H-4′, H-6′), 7.16 (dd, $J_{2,6}$ = 2.1 Hz, 1H, H-2), 7.00 (dd, $J_{6,2}$ = 2.1 Hz, $J_{6,5}$ = 8.1 Hz, 1H, H-6), 6.93 (d, $J_{5,6}$ = 8.1 Hz, 1H, H-5), 3.80 (s, 3H, OCH_3); EI MS *m/z* (% rel. abund.): 374 (M^+, 100), 373 (79), 358 (13), 357 (9), 343 (13), 330 (8).

2-Amino-4-(3-hydroxy-4-methoxyphenyl)-6-(phenylthio)pyridine-3,5-dicarbonitrile (10) [31]

Yellow Solid; Yield: 65%; M.P.: 215-217 °C; ^{1}H-NMR (400 MHz, DMSO-d_6) δ 9.42 (s, 1H, OH), 7.69 (s, 2H, NH), 7.60 (ovp, 2H, H-3′, H-5′), 7.49 (ovp, 3H, H-2′, H-4′, H-6′), 7.09 (d, $J_{6,5}$ = 8.0 Hz, 1H, H-6), 6.95 (ovp, 2H, H-2, H-5), 3.84 (s, 3H, OCH_3); EI MS *m/z* (% rel. abund.): 374 (M^+, 100), 373 (79), 357 (16), 343 (13), 327 (21), 303 (10), 282 (9).

2-Amino-4-(4-fluoro-3-methoxyphenyl)-6-(phenylthio)pyridine-3,5-dicarbonitrile (11)
CAS # 1353657-31-4

Intense Yellow Solid; Yield: 53%; M.P.: 193-195 °C; ^{1}H-NMR (300 MHz, DMSO-d_6) δ 7.81 (s, 2H, NH), 7.60 (ovp, 2H, H-3′, H-5′), 7.50 (ovp, 3H, H-2′, H-4′, H-6′), 7.45 (ovp, 2H, H-2, H-5), 7.16 (m, 1H, H-6); EI MS *m/z* (% rel. abund.): 376 (M^+, 100), 375 (88), 361 (29), 360 (34), 345 (61), 333 (23), 332 (45), 313 (11), 252 (8), 188 (15), 170 (10), 109 (14), 77 (15).

2-Amino-4-(4-hydroxy-3-iodo-5-methoxyphenyl)-6-(phenylthio)pyridine-3,5-dicarbonitrile (12)

Yellow Solid; Yield: 60%; M.P.: 245-247 °C; ^{1}H-NMR (400 MHz, DMSO-d_6) δ 10.17 (s, 1H, OH), 7.73 (s, 2H, NH), 7.58 (ovp, 2H, H-3′, H-5′), 7.49 (ovp, 4H, H-6, H-2′, H-4′, H-6′), 7.22 (s, 1H, H-2), 3.84 (s, 3H, OCH_3); ^{13}C-NMR (DMSO-d_6, 100 MHz): δ_C 165.9, 159.6, 156.9, 148.1, 146.5, 134.7, 134.7, 130.2, 129.6, 129.4, 129.4, 127.2, 126.2, 115.4, 115.1, 112.6, 93.4, 87.0, 84.3, 53.3; EI MS *m/z* (% rel. abund.): 500 (M^+, 1.2), 199 (10), 198 (100), 171 (5), 158 (3), 145 (2), 144 (8), 133 (2), 116(1), 92 (8), 67 (5), 66 (3)); HRESI-MS Calcd for $C_{20}H_{13}IN_4O_2S$: *m/z* = 499.9825, Found 499.9804.

2-Amino-4-(4-bromo-3,5-dimethoxyphenyl)-6-(phenylthio)pyridine-3,5-dicarbonitrile (13)

Light Yellow Solid; Yield: 62%; M.P.: 195-197 °C; ^{1}H-NMR (400 MHz, DMSO-d_6) δ 7.82 (s, 2H, NH), 7.60 (ovp, 2H, H-3′, H-5′), 7.50 (ovp, 3H, H-2′, H-4′, H-6′), 6.98 (s, 2H, H-1, H-6); ^{13}C-NMR (DMSO-d_6, 100 MHz): δ_C 165.9, 159.5, 157.9, 156.5, 156.5, 134.7, 134.7, 134.4, 134.4, 129.7, 129.4, 129.4, 115.2, 114.9, 105.4, 105.4, 101.8, 93.3, 87.1, 56.7, 56.7; EI MS *m/z* (% rel. abund.): 466 (M^+, 97), 468 (M+2, 100), 451 (6), 435 (14), 357 (5), 341 (5), 329 (10), 301 (8); HRESI-MS Calcd for $C_{21}H_{15}BrN_4O_2S$ *m/z* = 466.0069, Found 466.0099.

2-Amino-4-(2-bromo-4,5-dimethoxyphenyl)-6-(phenylthio)pyridine-3,5-dicarbonitrile (14)

Yellow Solid; Yield: 65%; M.P.: 230-232 °C; ^{1}H-NMR (400 MHz, DMSO-d_6) δ 7.86 (s, 2H, NH), 7.61 (ovp, 2H, H-3′, H-5′), 7.51 (ovp, 3H, H-2′, H-4′, H-6′), 7.33 (s, 1H, H-3), 7.17 (s, 1H, H-6), 3.85 (s, 3H, OCH_3), 3.76 (s, 3H, OCH_3); ^{13}C-NMR (DMSO-d_6, 100 MHz): δ_C 165.6, 159.3, 158.0, 150.4, 148.3, 134.8, 134.8. 129.7, 129.4, 129.4, 126.8, 126.6, 115.4, 114.6, 114.3, 112.8, 111.1, 94.3, 88.2, 56.0, 56.0; EI MS *m/z* (% rel. abund.): 466 (M^+, 100), 468 (M+2, 91), 371 (30), 343 (21), 329 (20), 301 (17), 278 (4), 231 (22), 229 (22), 203 (14), 172 (6), 110 (17), 109 (14), 83 (24) 44 (17); HRESI-MS Calcd for $C_{21}H_{15}BrN_4O_2S$ *m/z* = 466.0111, Found 466.0099.

2-Amino-4-(3-bromo-4,5-dimethoxyphenyl)-6-(phenylthio)pyridine-3,5-dicarbonitrile (15)

White Solid; Yield: 61%; M.P.: 228-230 °C; ^{1}H-NMR (400 MHz, DMSO-d_6) δ 7.89 (s, 2H, NH), 7.64 (ovp, 2H, H-3′, H-5′), 7.53 (ovp, 3H, H-2′, H-4′, H-6′), 7.36 (s, 1H, H-2), 7.19 (s, 1H, H-6), 3.88 (s, 3H, OCH_3), 3.79 (s, 3H, OCH_3); ^{13}C-NMR (DMSO-d_6, 100 MHz): δ_C 165.9, 159.5, 158.3, 150.2, 147.2, 134.8, 134.8, 129.7, 129.4, 129.4, 126.8, 126.3, 115.4, 114.5, 114.0, 113.7, 111.1, 94.7, 87.3, 56.0, 56.0; EI MS *m/z* (% rel. abund.): 466 (M^+, 100), 468 (M+2, 91), 371 (30), 343 (21), 329 (20), 301 (17), 278 (4), 231 (22), 229 (22); HRESI-MS Calcd for $C_{21}H_{15}BrN_4O_2S$ *m/z* = 466.0111, Found 466.0099.

2-Amino-6-(phenylthio)-4-(2,3,4-trimethoxyphenyl)pyridine-3,5-dicarbonitrile (16)

Light Yellow Solid; Yield: 70%; M.P.: 213-215 °C; ^{1}H-NMR (400 MHz, DMSO-d_6) δ 7.40 (s, 2H, NH), 7.61 (ovp, 2H, H-3′, H-5′), 7.49 (ovp, 3H, H-2′, H-4′, H-6′), 7.07 (s, 1H, H-6), 6.96 (s, 1H, H-5), 3.87 (s, 3H, OCH_3), 3.79 (s, 3H, OCH_3), 3.75 (s, 3H, OCH_3); ^{13}C-NMR (DMSO-d_6, 75 MHz): δ_C 159.4, 156.3, 155.2, 150.1, 134.8, 134.8, 129.6, 129.4, 129.4, 127.1, 127.1, 127.1, 124.2, 124.2, 120.2, 115.1, 114.8, 107.8, 94.5, 88.3, 61.2, 60.5, 55.9; EI MS *m/z* (% rel. abund.): 418 (M^+, 100), 417 (35), 403 (11), 387 (11), 371 (19), 354 (38), 343 (25), 329 (19), 317 (18), 294 (9), 144 (10); HRESI-MS Calcd for $C_{22}H_{18}N_4O_3S$ *m/z* = 418.1104, Found 418.1100.

2-Amino-6-(phenylthio)-4-(3,4,5-trimethoxyphenyl)pyridine-3,5-dicarbonitrile (17) [32]

Off White Solid; Yield: 62%; M.P.: 237-239 °C; ^{1}H-NMR (300 MHz, DMSO-d_6) δ 7.77 (s, 2H, NH), 7.60 (ovp, 2H, H-3′, H-5′), 7.50 (ovp, 3H, H-2′, H-4′, H-6′), 6.91 (s, 2H, H-1, H-6); EI MS *m/z* (% rel. abund.): 418 (M^+, 100), 403 (70), 343 (35), 331 (10), 317 (19), 300 (11), 289 (18), 172 (9).

2-Amino-4-(2,4-dimethoxyphenyl)-6-(phenylthio)pyridine-3,5-dicarbonitrile (18) [31]

Light Brown Solid; Yield: 60%; M.P.: 215-217 °C; ^{1}H-NMR (400 MHz, DMSO-d_6) δ 7.67 (s, 2H, NH), 7.60 (ovp, 2H, H-3′, H-5′), 7.49 (ovp, 3H, H-2′, H-4′, H-6′), 7.28 (d, $J_{6,5}$ = 8.4 Hz, 1H, H-6), 6.75 (d, $J_{3,5}$ = 2.0 Hz, 1H, H-3), 6.69 (dd, $J_{5,3}$ = 1.2 Hz, $J_{5,6}$ = 8.4 Hz, 1H, H-4); EI MS *m/z* (% rel. abund.): 389 (M^+, 55), 388 (100), 387 (75), 373 (10), 357 (25), 311 (65), 279 (7), 194 (11), 151 (9).

2-Amino-4-(3,4-dimethoxyphenyl)-6-(phenylthio)pyridine-3,5-dicarbonitrile (19) [33]

Off White Solid; Yield: 65%; M.P.: 262-264 °C; ^{1}H-NMR (400 MHz, DMSO-d_6) δ 7.72 (s, 2H, NH), 7.60 (ovp, 2H, H-3′, H-5′), 7.49 (ovp, 3H, H-2′, H-4′, H-6′), 7.19 (d, $J_{2,6}$ = 1.2 Hz, 1H, H-2), 7.12 (ovp, 2H, H-5, H-6); EI MS *m/z* (% rel. abund.): 388 (M^+, 100), 387 (27), 373 (7), 357 (8), 342 (7), 330 (6), 276 (8).

2-Amino-4-(3,5-dimethoxyphenyl)-6-(phenylthio)pyridine-3,5-dicarbonitrile (20)

Reddish Brown Solid; Yield: 62%; M.P.: 223-225 °C; ^{1}H-NMR (400 MHz, DMSO-d_6) δ 7.76 (s, 2H, NH), 7.60 (ovp, 2H, H-3′, H-5′), 7.50 (ovp, 3H, H-2′, H-4′, H-6′), 6.68 (ovp, 3H, H-2, H-4, H-6), 3.79 (s, 6H, OCH_3); ^{13}C-NMR (DMSO-d_6, 75 MHz): δ_C 165.9, 160.4, 159.5, 158.3, 158.3, 135.6, 134.8, 134.8, 129.6, 129.4, 129.4, 127.1, 127.1, 115.1, 114.8, 106.5, 106.5, 101.6, 93.3, 87.0, 55.4, 55.4; EI MS *m/z* (% rel. abund.): 388 (M^+, 100), 357 (19), 342 (3), 329 (5), 276 (2), 194 (4), 165 (3), 151 (1), 109 (1), 77 (2); HRESI-MS Calcd for $C_{22}H_{18}N_4O_3S$ *m/z* = 388.0093, Found 388.0094.

2-Amino-4-(4-ethoxy-3-methoxyphenyl)-6-(phenylthio)pyridine-3,5-dicarbonitrile (21)

White Solid; Yield: 65%; M.P.: 223-225 °C; ^{1}H-NMR (400 MHz, DMSO-d_6) δ 7.71 (s, 2H, NH), 7.60 (ovp, 2H, H-3′, H-5′), 7.49 (ovp, 3H, H-2′, H-4′, H-6′), 7.19 (d, $J_{2,6}$ = 1.6 Hz, 1H, H-2), 7.10 (m, 2H, H-5, H-6), 4.12 (q, $J_{CH2,CH3}$ = 6.8 Hz, 2H, CH_2), 3.79 (s, 3H, OCH_3), 1.37 (t, $J_{CH3,CH2}$ = 6.8 Hz, 3H, OCH_3); ^{13}C-NMR (DMSO-d_6, 125 MHz): δ_C 166.0, 159.7, 158.3, 149.6, 148.3, 134.7, 134.7, 129.6, 129.4, 129.4, 127.2, 125.6, 121.5, 115.5, 115.2, 112.4, 112.2, 63.7, 55.6, 14.6; EI MS *m/z* (% rel. abund.): 402 (M^+, 100), 373 (61), 358 (8), 343 (10), 330 (6), 313 (5), 276 (5); HRESI-MS Calcd for $C_{22}H_{18}N_4O_2S$ *m/z* = 402.1145, Found 402.1150.

2-Amino-4-(naphthalen-1-yl)-6-(phenylthio)pyridine-3,5-dicarbonitrile (22) [34]

Solid Brown Crystalline; Yield: 65%; M.P.: 295-297 °C; ^{1}H-NMR (400 MHz, DMSO-d_6) δ 8.13 (d, $J_{9,8}$ = 8.0 Hz, 1H, H-9), 8.07 (d, $J_{2,3}$ = 7.6 Hz, 1H, H-2), 7.69 (ovp, 3H, H-4, H-3′, H-5′), 7.62 (ovp, 4H, H-3, H-6, H-7, H-8), 7.50 (ovp, 3H, H-2′, H-4′, H-6′); EI MS *m/z* (% rel. abund.): 378 (M^+, 89), 377 (100), 345 (7), 301 (7), 269 (3), 215 (8), 188 (8).

2-Amino-4-(naphthalen-2-yl)-6-(phenylthio)pyridine-3,5-dicarbonitrile (23) [35]

Yellow Solid; Yield: 68%; M.P.: 315-317 °C; ^{1}H-NMR (400 MHz, DMSO-d_6) δ 8.15 (s, 1H, H-4), 8.12 (s, 1H, H-7), 8.06 (m, 2H, H-9, H-10), 7.84 (s, 2H, NH), 7.68 (ovp, 5H, H-2′, H-3′, H-4′, H-5′, H-6′), 7.51 (ovp, 3H, H-2, H-5, H-6); EI MS *m/z* (% rel. abund.): 378 (M^+, 100), 377 (98), 334 (5), 215 (5), 189 (8), 160 (9), 147 (7).

2-Amino-4-(3-(benzyloxy)-4-methoxyphenyl)-6-(phenylthio)pyridine-3,5-dicarbonitrile (24)

Yellow Solid; Yield: 67%; M.P.: 225-227 °C; ^{1}H-NMR (400 MHz, DMSO-d_6) δ 7.73 (s, 2H, NH), 7.60 (ovp, 2H, H-3′, H-5′), 7.49 (ovp, 4H, H-2′, H-4′, H-6′, H-5), 7.41 (t, $J_{9(8,10)} = J_{10(9,11)} = J_{11(12,10)}$ = 7.6 Hz, 3H, H-9, H-10, H-11), 7.36 (ovp, 2H, H-8, H-12), 7.18 (ovp, 2H, H-5, H-6), 5.07 (s, 1H, CH_2), 3.84 (s, 3H, OCH_3); ^{13}C-NMR (DMSO-d_6, 125 MHz): δ_C 166.0, 159.7, 158.2, 150.7, 147.5, 136.6, 134.8, 134.8, 129.6, 129.4, 129.4, 128.4, 128.4, 128.0, 127.9,127.9, 127.2, 125.8, 122.0, 115.5, 115.2, 113.9, 111.8, 70.4, 55.6; EI MS *m/z* (% rel. abund.): 464 (M^+, 63), 447 (10), 433 (16), 374 (33), 360 (55), 342 (11), 302 (9), 276 (12), 92 (26), 91 (100); HRESI-MS Calcd for $C_{27}H_{20}N_4O_2S$ *m/z* = 464.1287, Found 464.1307.

2-Amino-4-(4-(benzyloxy)phenyl)-6-(phenylthio)pyridine-3,5-dicarbonitrile (25) CAS # 1019063-42-3

White Solid; Yield: 62%; M.P.: 207-209 °C; ^{1}H-NMR (400 MHz, DMSO-d_6) δ 7.73 (s, 2H, NH), 7.60 (ovp, 2H, H-2, H-6), 7.52 (ovp, 7H, H-2′, H-3′, H-4′, H-5′, H-6′, H-8, H-12), 7.43 (t, $J_{9(10,8)} = J_{11(10,12)}$ = 7.2 Hz, 2H, H-9, H-11), 7.36 (t, $J_{10(11,9)}$ = 7.2 Hz, 1H, H-10), 7.20 (d, $J_{3,2} = J_{5,6}$ = 8.8 Hz, 2H, H-3, H-5), 5.18 (s, 2H, CH_2); EI MS *m/z* (% rel. abund.): 434 (M^+, 78), 343 (10), 314 (4), 288 (2), 92 (15), 91 (100), 65 (7).

2-Amino-4-(2-chlorophenyl)-6-(phenylthio)pyridine-3,5-dicarbonitrile (26) CAS # 1414218-12-4

White Solid; Yield: 63%; M.P.: 235-237 °C; ^{1}H-NMR (400 MHz, DMSO-d_6) δ 7.93 (s, 2H, NH), 7.70 (d, $J_{6,5}$ = 8.0 Hz, 1H, H-6), 7.62 (ovp, 3H, H-3, H-4, H-5), 7.59 (ovp, 2H, H-3′, H-5′), 7.50 (ovp, 3H, H-2′, H-4′, H-6′); EI MS *m/z* (% rel. abund.): 362 (M^+, 100), 361 (91), 328 (23), 327 (87), 326 (11), 325 (6), 310 (6), 299 (6), 218 (5), 163 (4), 136 (2), 109 (7), 77 (7).

2-Amino-4-(4-chlorophenyl)-6-(phenylthio)pyridine-3,5-dicarbonitrile (27) [36]

Solid Light Yellow Crystalline; Yield: 65%; M.P.: 230-232 °C; ^{1}H-NMR (300 MHz, DMSO-d_6) δ 7.84 (s, 2H, NH), 7.67 (d, $J_{2,3}$ = $J_{6,5}$ = 11.2 Hz, 2H, H-2, H-6), 7.60 (ovp, 4H, H-3, H-5, H-3′, H-5′), 7.50 (ovp, 3H, H-2′, H-4′, H-6′); EI MS *m/z* (% rel. abund.): 364 (M^+, 31), 362 (M+2, 100), 361 (83), 327 (23), 318 (4), 199 (17), 163 (9), 109 (7), 77 (14), 65 (5), 50 (16).

2-Amino-4-(2-chloro-3-methoxyphenyl)-6-(phenylthio)pyridine-3,5-dicarbonitrile (28)

White Solid; Yield: 45%; M.P.: 305-307 °C; ^{1}H-NMR (400 MHz, DMSO-d_6) δ 7.90 (s, 2H, NH), 7.62 (ovp, 2H, H-3′, H-5′), 7.52 (ovp, 4H, H-6, H-2′, H-4′, H-6′), 7.34 (d, $J_{5,4}$ = 8.0 Hz, 1H, H-5), 7.09 (d, $J_{4,5}$ = 8.0 Hz, 1H, H-5), 3.93 (s, 3H, OCH_3); ^{13}C-NMR (DMSO-d_6, 75 MHz): δ_C 165.9, 159.3, 156.4, 154.8, 134.8, 134.8, 134.2, 129.8, 129.4, 129.4, 128.6, 126.7, 121.2, 119.0, 114.4, 114.1, 114.0, 93.5, 87.6, 56.3; EI MS *m/z* (% rel. abund.): 392 (M^+, 100), 376 (4), 357 (42), 342 (22), 326 (7), 314 (18), 286 (3), 248 (2), 109 (3), 77 (3); HRESI-MS Calcd for $C_{20}H_{13}ClN_4OS$ *m/z* = 392.0479, Found 392.0499.

Molecular Docking Study

To prepare a homology model of α-glucosidase, we used the method described by Imran et al. [37, 38]. At first, a search was carried out using SWISS-MODEL to identify a protein in the PDB with a high sequence similarity with *S. cerevisiae* α-glucosidase. As a result, isomaltase from *S. cerevisiae* (PDB code 3A4A), with 72% identical and shares 85% similarity with the *S. cerevisiae* α-glucosidase, was selected. Next, this enzyme was subjected through sequence alignment and homology model using automated homology modeling pipeline SWISS-MODEL (managed by Swiss Institute of Bioinformatics) and the quality of the obtained homology model was verified using PROCHECK [39]. The 3D structures of the acarbose and selected synthesized inhibitors were built by MarvineSketch 5.8.3, 2012, ChemAxon (http://www.chemaxon.com) and converted

to pdbqt coordinate using Auto dock Tools. The pdbqt coordinate of modeled *α*-glucosidase was produced using the same software. Also, the pdbqt coordinate of protein was procured using the Auto Dock Tools. The water molecules and the inhibitors were removed from protein. Then, using Auto Dock Tools, polar hydrogen atoms were added, Koullman charges were assigned, and the obtained protein structure was used as an input file for the AUTOGRID program. In AUTOGRID for each atom type in the ligand, maps were calculated with 0.375 Å spacing between grid points and the center of the grid box was placed at x = 12.5825, y = −7.8955, z = 12.519. The dimensions of the active site box were set at 40 × 40 × 40 Å. Flexible ligand dockings were accomplished for the selected compounds. Each docked system was carried out by 50 runs of the AUTODOCK search by the Lamarckian genetic algorithm (LGA). The best poses of the selected compounds were selected for analyzing the interactions between enzyme and the inhibitors. The results were visualized using BIOVIA Discovery Studio v.3.5.

Acknowledgement: The authors are thankful to the Pakistan Academy of Sciences for providing financial support to Project No. (5-9/PAS/440).

References

[1] R. Tundis, M. Loizzo, F. Menichini, Natural products as *α*-amylase and *α*-glucosidase inhibitors and their hypoglycaemic potential in the treatment of diabetes: an update, Mini Reviews in Medicinal Chemistry, 10 (2010) 315-331.

[2] A. Kimura, Molecular anatomy of *α*-glucosidase, Trends in Glycoscience and Glycotechnology, 12 (2000) 373-380.

[3] H. Chen, K. Ouyang, Y. Jiang, Z. Yang, W. Hu, L. Xiong, N. Wang, X. Liu, W. Wang, Constituent analysis of the ethanol extracts of *Chimonanthus nitens* Oliv. leaves and their inhibitory effect on *α*-glucosidase activity, International Journal of Biological Macromolecules, 98 (2017) 829-836.

[4] S. Kasturi, S. Surarapu, S. Uppalanchi, J.S. Anireddy, S. Dwivedi, H.S. Anantaraju, Y. Perumal, D.K. Sigalapalli, B.N. Babu, K.S. Ethiraj, Synthesis and *α*-glucosidase inhibition activity of dihydroxy pyrrolidines, Bioorganic & Medicinal Chemistry Letters, 27 (2017) 2818-2823.

[5] M. Yar, M. Bajda, S. Shahzad, N. Ullah, M.A. Gilani, M. Ashraf, A. Rauf, A. Shaukat, Organocatalyzed solvent free an efficient novel synthesis of 2, 4, 5-trisubstituted imidazoles for *α*-glucosidase inhibition to treat diabetes, Bioorganic Chemistry, 58 (2015) 65-71.

[6] N. Asano, Glycosidase inhibitors: update and perspectives on practical use, Glycobiology, 13 (2003) 93R-104R.

[7] E. Nagai, T. Katsuno, J.-i. Miyagawa, K. Konishi, M. Miuchi, F. Ochi, Y. Kusunoki, M. Tokuda, K. Murai, T. Hamaguchi, Effects of miglitol in combination with intensive insulin therapy on blood glucose control with special reference to incretin responses in type 1 diabetes mellitus, Endocrine Journal, (2011) 1108100603.

[8] E. Buschur, F. Brown, J. Wyckoff, Using oral agents to manage gestational diabetes: what have we learned?, Current Diabetes Reports, 15 (2015) 4.

[9] M. Hanefeld, M. Cagatay, T. Petrowitsch, D. Neuser, D. Petzinna, M. Rupp, Acarbose reduces the risk for myocardial infarction in type 2 diabetic patients: meta-analysis of seven long-term studies, European Heart Journal, 25 (2004) 10-16.

[10] M.M. Rosa, T. Dias, Commonly used endocrine drugs, in: Handbook of Clinical Neurology, Elsevier, 2014, pp. 809-824.

[11] M. Ajaib, S. Fatima, S.H. Kamran, K.M. Khan, S. Perveen, S. Shah, Comprative antidiabetic evaluation of different parts of *Nicotiana plumbajnifolia* in alloxan induced diabetic mice, Journal of Chemical Society of Pakistan, 38 (2016) 1267-1270.

[12] M. Ajaib, M. Latif, S.H. Kamran, K.M. Khan, S. Perveen, S. Shah, A. Karim, Comparative anti-diabetic evaluation of different parts of *Himalrandia tetrasperma* in alloxan induced diabetic in mice, Journal of Chemical Society of Pakistan, 38 (2016) 313-317.

[13] S. Perveen, S. Mustafa, K. M. Khan, M. I. Choudhary, 1,3-disubstituted ureas as antiglycating agents, Journal of the Chemical Society of Pakistan, 35 (2013) 1603-1611.

[14] M.A. Abbasi, S.A.H. Shah, Aziz-ur-Rehman, S.Z. Siddiqui, G. Hussain, K.M. Khan, M. Ashraf, S.A. Ejaz, Synthesis of (*E*)-*N*'-[1-(2,4-dihydroxyphenyl)ethylidene]substituted

hydrazides as possible *α*-glucosidase and butyrylcholinesterase inhibitors, Journal of Chemical Society of Pakistan, 39 (2017) 248-253.

[15] A. Mollica, G. Zengin, A. Stefanucci, C. Ferrante, L. Menghini, G. Orlando, L. Brunetti, M. Locatelli, M.P. Dimmito, E. Novellino, O.K. Wakeel, Nutraceutical potential of *Corylus avellana* daily supplements for obesity and related dysmetabolism. Journal of Functional Foods, 47 (2018) 562-574.

[16] A. Mollica, G. Zengin, S. Durdagi, R. E. Salmas, G. Macedonio, A. Stefanucci, M.P. Dimmito, E. Novellino, Combinatorial peptide library screening for discovery of diverse *α*-glucosidase inhibitors using molecular dynamics simulations and binary QSAR models. Journal of Biomolecular Structure and Dynamics, 37 (2019) 726-740.

[17] D.W. Hopper, A.L. Crombie, J.J. Clemens, S. Kwon, .1: Six-membered ring systems: pyridine and benzo derivatives, in: Progress in Heterocyclic Chemistry, Elsevier, 2009, pp. 330-374.

[18] P.E. Chabrier, P. Guinot, T. Tarrade, M. Auguet, M. Cabanie, F. Clostre, A. Etienne, A. Esanu, P. Braquet, Cicletanine, Cardiovascular Drug Reviews, 6 (1988) 166-179.

[19] J.W. Pape, S.S. Jean, J.L. Ho, A. Hafner, W.D. Johnson Jr, Effect of isoniazid prophylaxis on incidence of active tuberculosis and progression of HIV infection, The Lancet, 342 (1993) 268-272.

[20] H. Niaz, H. Kashtoh, J.A. Khan, A. Khan, M.T. Alam, K.M. Khan, S. Perveen, M.I. Choudhary, Synthesis of diethyl 4-substituted-2,6-dimethyl-1,4-dihydropyridine-3,5-dicarboxylates as a new series of inhibitors against yeast *α*-glucosidase, European Journal of Medicinal Chemistry, 95 (2015) 199-209.

[21] F. Ali, K.M. Khan, U. Salar, M. Taha, N.H. Ismail, A. Wadood, M. Riaz, S. Perveen, Hydrazinyl arylthiazole based pyridine scaffolds: Synthesis, structural characterization, *in vitro α*-glucosidase inhibitory activity, and *in silico* studies, European Journal of Medicinal Chemistry, 138 (2017) 255-272.

[22] a) M. Taha, N.H. Ismail, S. Imran, I. Ainaa, M. Selvaraj, M. Ali, K.M. Khan, N. Uddin, Synthesis of 2-phenyl-1*H*-imidazo [4,5-b] pyridine as type 2 diabetes inhibitors and

molecular docking studies, Medicinal Chemistry Research, 26 (2017) 916-928. b) G. Ahad, M. Khan, A. Khan, M. Ibrahim, U. Salar, Kanwal, K. M. Khan, S. Perveen, Synthesis, structural characterization, and antioxidant activities of 2,4-dinitrophenyl-hydrazone derivatives, Journal of Chemical Society of Pakistan, **2018**, *40*, 961-973.

[23] M. Taha, N.H. Ismail, S. Imran, H. Rashwan, W. Jamil, S. Ali, S.M. Kashif, F. Rahim, U. Salar, K.M. Khan, Synthesis of 6-chloro-2-aryl-1*H*-imidazo [4, 5-b] pyridine derivatives: Antidiabetic, antioxidant, *β*-glucuronidase inhibiton and their molecular docking studies, Bioorganic Chemistry, 65 (2016) 48-56.

[24] M. Taha, M.T. Javid, S. Imran, M. Selvaraj, S. Chigurupati, H. Ullah, F. Rahim, F. Khan, J.I. Mohammad, K.M. Khan, Synthesis and study of the *α*-amylase inhibitory potential of thiadiazole quinoline derivatives, Bioorganic Chemistry, 74 (2017) 179-186.

[25] M. Adib, F. Peytam, M. Rahmanian-Jazi, S. Mahernia, H.R. Bijanzadeh, M. Jahani, M. Mohammadi-Khanaposhtani, S. Imanparast, M.A. Faramarzi, M. Mahdavi, New 6-amino-pyrido [2, 3-d] pyrimidine-2,4-diones as novel agents to treat type 2 diabetes: a simple and efficient synthesis, *α*-glucosidase inhibition, molecular modeling and kinetic study, European Journal of Medicinal Chemistry, 155 (2018) 353-363.

[26] M. Thimmaiah, P. Li, S. Regati, B. Chen, J.C.-G. Zhao, Multi-component synthesis of 2-amino-6-(alkylthio) pyridine-3, 5-dicarbonitriles using Zn (II) and Cd (II) metal-organic frameworks (MOFs) under solvent-free conditions, Tetrahedron Letters, 53 (2012) 4870-4872.

[27] M.N. Khan, S. Pal, T. Parvin, L.H. Choudhury, A simple and efficient method for the facile access of highly functionalized pyridines and their fluorescence property studies, RSC Advances, 2 (2012) 12305-12314.

[28] S. Banerjee, G. Sereda, One-step, three-component synthesis of highly substituted pyridines using silica nanoparticle as reusable catalyst, Tetrahedron Letters, 50 (2009) 6959-6962.

[29] J.B. Gujar, M.A. Chaudhari, D.S. Kawade, M.S. Shingare, Sodium chloride: A proficient additive for the synthesis of pyridine derivatives in aqueous medium, Tetrahedron Letters, 55 (2014) 6939-6942.

[30] S. Mishra, R. Ghosh, K_2CO_3-mediated, one-pot, multicomponent synthesis of medicinally potent pyridine and chromeno [2, 3-b] pyridine scaffolds, Synthetic Communications, 42 (2012) 2229-2244.

[31] N.M. Evdokimov, A.S. Kireev, A.A. Yakovenko, M.Y. Antipin, I.V. Magedov, A. Kornienko, One-step synthesis of heterocyclic privileged medicinal scaffolds by a multicomponent reaction of malononitrile with aldehydes and thiols, The Journal of Organic Chemistry, 72 (2007) 3443-3453.

[32] N.M. Evdokimov, I.V. Magedov, A.S. Kireev, A. Kornienko, One-step, three-component synthesis of pyridines and 1, 4-dihydropyridines with manifold medicinal utility, Organic letters, 8 (2006) 899-902.

[33] A. Nakhaei, H. Nakhaei, Fe_3O_4@ GO-Pr-SO_3H as an efficient and recyclable catalyst for the synthesis of pyridine dicarbonitriles, Heterocyclic Letters, 8 (2018) 27-33.

[34] R. Mamgain, R. Singh, D.S. Rawat, DBU-catalyzed three-component one-pot synthesis of highly functionalized pyridines in aqueous ethanol, Journal of Heterocyclic Chemistry, 46 (2009) 69-73.

[35] S. Sobhani, M. Honarmand, 2-Hydroxyethylammonium acetate: A reusable task-specific ionic liquid promoting one-pot, three-component synthesis of 2-amino-3, 5-dicarbonitrile-6-thio-pyridines, Comptes Rendus Chimie, 16 (2013) 279-286.

[36] P.V. Shinde, S.S. Sonar, B.B. Shingate, M.S. Shingare, Boric acid catalyzed convenient synthesis of 2-amino-3, 5-dicarbonitrile-6-thio-pyridines in aqueous media, Tetrahedron Letters, 51 (2010) 1309-1312.

[37] S. Imran, M. Taha, N.H. Ismail, S.M. Kashif, F. Rahim, W. Jamil, M. Hariono, M. Yusuf, H. Wahab, Synthesis of novel flavone hydrazones: *In vitro* evaluation of α-glucosidase inhibition, QSAR analysis and docking studies, European Journal of Medicinal Chemistry, 105 (2015) 156-170.

[38] S. Imran, M. Taha, N.H. Ismail, S.M. Kashif, F. Rahim, W. Jamil, H. Wahab, K.M. Khan, Synthesis, *in vitro* and docking studies of new flavone ethers as α-glucosidase inhibitors, Chemical Biology & Drug Design, 87 (2016) 361-373.

[39] F. Kiefer, K. Arnold, M. Künzli, L. Bordoli, T. Schwede, The SWISS-MODEL Repository and associated resources, Nucleic Acids Research, 37 (2009) D387-D392.

Synthesis, *In vitro* and *In silico* Screening of 2-Amino-4-Aryl-6-(phenylthio) pyridine-3,5-dicarbonitriles as Novel α-Glucosidase Inhibitors

Muhammad Ali, Khalid Mohammed Khan,* Mohammad Mahdavi, Abdul Jabbar, Shahbaz Shamim, Uzma Salar, Muhammad Taha, Shahnaz Parveen, Bagher Larijani, Mohammad Ali Faramarzi

H. E. J. Research Institute of Chemistry, International Center for Chemical and Biological Sciences, University of Karachi, Karachi-75270, Pakistan

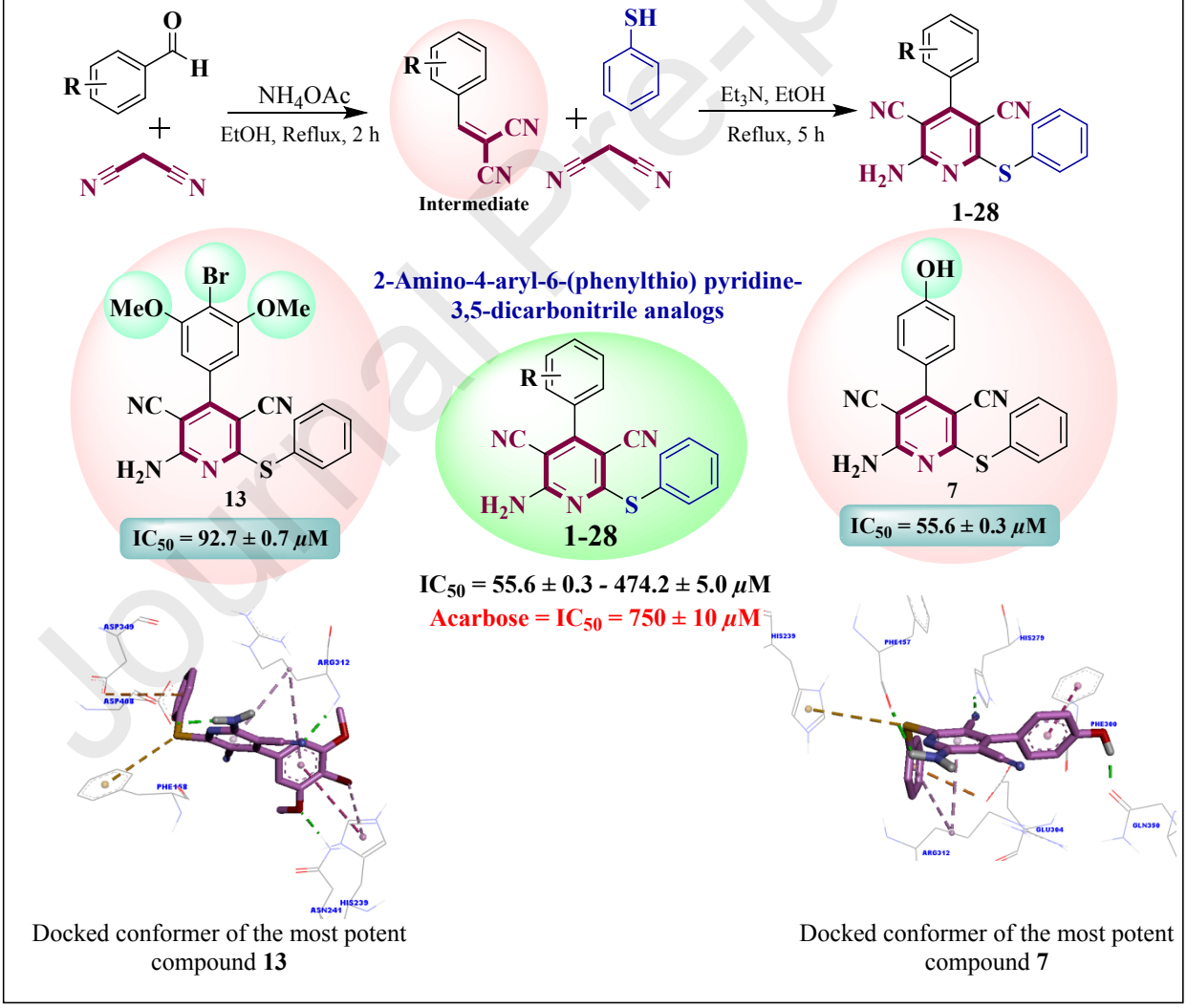

Docked conformer of the most potent compound **13**

Docked conformer of the most potent compound **7**

Highlights:

- 2-Amino-4-aryl-6-(phenylthio)pyridine-3,5-dicarbonitriles **1-28** were synthesized.
- Compounds were subjected to *in vitro* α-glucosidase inhibitory activity.
- Compounds **1**-**3**, **7**, **9**, **11-14**, and **16** showed many folds increased inhibitory potential.
- Structure-activity relationship (SAR) was established.
- Kinetic studies showed the competitive type inhibitory mechanism by the most potent molecule **7**.
- *In silico* study was performed to decipher the binding interaction of compound **7** with the active pocket of α-glucosidase enzyme.